

Magnetic nanocomposite catalysts for hydrogenation of organic compounds

Svetlana I. Pomogailo,^{a,b} Evgeny G. Chepaikin,^{a,†} Olga P. Tkachenko,^c Olga N. Bubelo,^b Rosa I. Jussupkaliyeva^d and Leonid M. Kustov^{*c,e}

^a A. G. Merzhanov Institute of Structural Macrokinetics and Materials Science, Russian Academy of Sciences, 142432 Chernogolovka, Moscow Region, Russian Federation

^b Russian Institute for Scientific and Technical Information, Russian Academy of Sciences, 125190 Moscow, Russian Federation

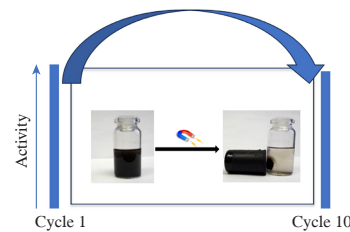
^c N. D. Zelinsky Institute of Organic Chemistry, Russian Academy of Sciences, 119991 Moscow, Russian Federation. Fax: +7 499 137 2935; e-mail: lmk@ioc.ac.ru

^d Zhangir Khan West Kazakhstan Agrarian Technical University, 090009 Uralsk, Kazakhstan

^e Department of Chemistry, M. V. Lomonosov Moscow State University, 119991 Moscow, Russian Federation

DOI: 10.71267/mencom.7645

This brief review examines hydrogenation reactions catalyzed by magnetite-based nanocomposite catalysts. It is shown that these catalysts are environmentally friendly, recyclable and, due to the presence of magnetite in their composition, easily separated from the reaction medium.



Keywords: nanocatalysts, magnetite, hydrogenation, furfural, furfuryl alcohol, benzaldehyde, 4-nitrophenol, benzyl alcohol, 4-aminophenol.

Introduction

In recent years, interest in the use of iron-based catalysts and nanomaterials, especially magnetically separable catalysts, has not diminished due to their unique properties and the possibility of reuse.^{1–32} Magnetic materials are easily separated from the reaction medium using an external magnetic field, which eliminates cumbersome filtration and centrifugation operations. In particular, magnetite nanoparticles are used as a catalyst carrier.^{2–30} In some cases, magnetite nanoparticles are active centers in catalytic processes.^{1,4,10}

The methods of their preparation have a great influence on the formation of the composite structure. The introduction of magnetite nanoparticles is usually carried out in two ways: *ex situ* (when pre-synthesized magnetite is used) or *in situ*, *i.e.* with the formation of magnetite nanoparticles at the time of nanocomposite synthesis. A number of studies using various modern physico-chemical methods (IR-Fourier spectroscopy, electron microscopy, X-ray diffraction, X-ray fluorescence analysis, *etc.*) have shown the formation of nanocomposites with a core–shell structure, which affects their catalytic properties and stability. The introduction of a second doping metal is also

of great importance for improving the catalytic properties of magnetic nanocomposites.

This review examines examples of reactions in which the use of magnetite-containing nanocatalysts is promising. The review also analyzes the applications of chemically modified magnetite nanoparticles in the catalysis of various reactions. This review will consider works published in the period from 2019 to 2024. The structure of the mini-review is built on the analysis of traditional reactions of reduction/hydrogenation of nitroarenes and nitrophenols with a further shift to hot reactions, such as furfural hydrogenation, use for hydrogen storage and CO₂ utilization.

Let us first define the term ‘magnetic nanocomposites’ as materials that meet all of the following criteria: (1) they are magnetic, (2) they are nanometer-sized particles, and (3) they contain at least two (or more) components, each of which is nanometer-sized. Thus, all core–shell materials with magnetic nanoparticles used as cores or as decorating nanoparticles belong to this class.

There are three main types of magnetic nanocomposite materials reported in the literature. (A) The first type includes systems in which the magnetic phase is active in the reaction under consideration, such as the reduction of nitrophenol with sodium borohydride, hydrogenation of furfural, hydrogenation of CO₂ and reduction of oxygen. (B) The second type consists of

[†] Deceased.

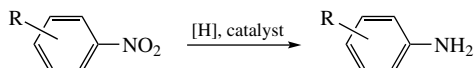
systems that contain active metal nanoparticles supported on magnetic nanoparticles. Examples include composites consisting of Pd or Ni nanoparticles supported on magnetite nanoparticles and active in benzaldehyde hydrogenation. (C) The third type of materials contains magnetic nanoparticles as cores coated with one or two shells (porous or not). In this case, the magnetic nanoparticles can be active or inactive in the catalyzed reaction.

Such magnetic nanoparticles have certain advantages and disadvantages compared to supported non-magnetic materials used in catalytic reduction or hydrogenation reactions. The advantages include the possibility of multiple (5–10 times) separation from the reaction medium without loss of activity, their non-toxicity, low cost and availability, as well as the ease of preparing these materials. However, they also have some disadvantages, such as leaching of active components, a decrease in saturation magnetization compared to the bulk magnetite, limited accessibility of active sites due to diffusion through the shells, complex composition and structure of these nanomaterials, a decrease in activity and specific surface area, and, finally, a limited number of magnetic compounds with acceptable characteristics. Nevertheless, the advantages of such magnetic nanocatalysts have prompted their wide application in liquid-phase reactions, which will be discussed below.

Reduction of nitroarenes

The reduction of nitroarenes allows producing a variety of amines (Scheme 1), which are intermediate products for use in synthesis and industry in the production of dyes, pigments, pharmaceuticals, synthetic polymers and agrochemicals, including pesticides, *etc.*

Magnetically separable $\text{Fe}_3\text{O}_4@\text{NC}/\text{Pd}$ catalysts based on Pd nanoparticles embedded in Fe_3O_4 coated with nitrogen-modified



Scheme 1 Reduction of nitroarenes to aminoarenes.



Svetlana I. Pomogailo, Cand. Sci. (Chem. Sci.), Senior Research Scientist, A. G. Merzhanov Institute of Structural Macrokinetics and Materials Science, Russian Academy of Sciences, Chernogolovka, Moscow Region, All-Russian Institute for Scientific and Technical Information (VINITI RAS), Moscow, Russian Federation. ORCID: <https://doi.org/0000-0001-8200-0706>. E-mail: pomogsvetlana@mail.ru. Field of interests: polymers, nanocomposites, synthesis, homogeneous catalysis, heterogeneous catalysis and noble metal catalysts.

Evgeny G. Chepaikin, Cand. Sci. (Chem. Sci.), Leading Researcher, A. G. Merzhanov Institute of Structural Macrokinetics and Materials Science of Russian Academy of Sciences (ISMAN). ORCID: <https://doi.org/0000-0002-1631-021X>. E-mail: echev@ism.ac.ru. Field of interests: kinetics and mechanism of gas- and liquid-phase catalytic reactions, homogeneous and heterogeneous catalysis, metal-complex catalytic systems and catalysts based on noble metals.



Olga P. Tkachenko, Cand. Sci. (Chem. Sci.), Senior Research Scientist, N. D. Zelinsky Institute of Organic Chemistry, Russian Academy of Sciences, Moscow. ORCID: <https://orcid.org/0000-0002-2673-0453>. E-mail: ot@ioc.ac.ru. Field of interests: preparation and characterization of catalysts by TPR, XPS, XAS and DRIFTS methods.



Olga N. Bubelo, Cand. Sci. (Chem. Sci.), Senior Research Scientist, Head of the Department of Scientific Information on Problems of Chemistry and Material Science, All-Russian Institute for Scientific and Technical Information (VINITI RAS), Moscow, Russian Federation. E-mail: bon199@yandex.ru. Field of interests: photochemical reactions, photocatalysis, laser chemistry, inorganic materials and ‘green’ chemistry.



Roza I. Jussupkaliyeva, Master of Technical Sciences, Senior Lecturer, Zhangir Khan West Kazakhstan Agrarian Technical University. ORCID: <https://doi.org/0000-0001-8916-0008>. E-mail: rozaid2@mail.ru. Field of interests: inorganic materials, composites, catalysis, petrochemistry and oxidation of alkanes.



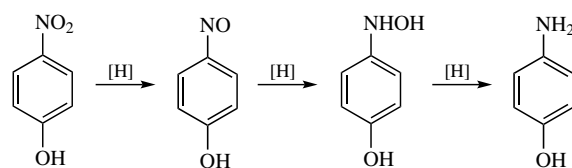
Leonid M. Kustov is the Head of the Laboratory of Development and Study of Polyfunctional Catalysts at the N. D. Zelinsky Institute of Organic Chemistry, Russian Academy of Science, and the Head of the Laboratory of Ecological Chemistry at the Chemistry Department of the M. V. Lomonosov Moscow State University. He is Doctor of Chemical Sciences, Professor. He is an expert in the areas of physical chemistry, catalysis and petrochemistry. He has about 600 publications, including 70 reviews and 100 inventions.

carbon were prepared for the hydrogenation of various substituted nitroarenes.² These materials were obtained from various types of biomass and biomass-derived products (chitosan and glucosamine) as carbon and nitrogen sources. To synthesize the catalyst with the ‘magnetic core–shell’ structure, Fe_3O_4 particles were preliminarily prepared *ex situ* in solution, which were then subjected to hydrothermal treatment together with chitosan or glucosamine. As a result, glucosamine or chitosan was converted into a carbon shell around Fe_3O_4 , forming $\text{Fe}_3\text{O}_4@\text{NC}$ spheres. Then, Pd^{2+} ions were adsorbed on the $\text{Fe}_3\text{O}_4@\text{NC}$ surface, where they were reduced with ascorbic acid, providing a Pd content of 5.1 wt%. It was noted that $\text{Fe}_3\text{O}_4@\text{NC}/\text{Pd}$ disperses well in water, which facilitates the interaction of the substrate with the active centers of the catalyst, as well as the subsequent separation of magnetic particles from the reaction solution. Catalysts based on $\text{Fe}_3\text{O}_4@\text{NC}/\text{Pd}$ showed high catalytic activity and chemoselectivity in the hydrogenation reactions of various substituted nitroarenes, including those containing reducible functional groups, to the corresponding aromatic amines in an aqueous medium. The catalysts can be easily separated and reused in at least eight cycles without visible loss of catalytic properties.

Reduction of 4-nitrophenol

The reduction of 4-nitrophenol with sodium borohydride or hydrazine hydrate is another important reaction catalyzed by magnetite-based catalysts (Scheme 2).

A $\text{Fe}_3\text{O}_4/\text{pectin}/\text{Au}$ nanocomposite consisting of pectin-modified magnetite decorated with Au nanoparticles was



Scheme 2 Stages of reduction of 4-nitrophenol to 4-aminophenol with sodium borohydride or hydrazine hydrate.

synthesized and characterized.³ Its synthesis involved coating previously obtained magnetite with pectin to yield Fe_3O_4 /pectin. When adding a HAuCl_4 solution to the Fe_3O_4 –pectin system at pH 11, Au^{3+} is reduced to Au^0 *in situ* due to the hydroxyl groups of pectin. Thus, the pectin shell serves not only as a protective shell for Fe_3O_4 nanoparticles, but also as an environmentally friendly reducing agent in the synthesis of Au nanoparticles *in situ*. In addition, the polar environment created by the biopolymer promotes dispersion of surface Au nanoparticles, thereby suppressing their self-aggregation. The nanocomposite was used as a catalyst for the reduction of nitroarenes using $\text{N}_2\text{H}_4 \cdot \text{H}_2\text{O}$ as a reducing agent in ethanol–water medium without the use of promoters or ligands. It was shown that the Fe_3O_4 /pectin/Au system contributes to achieving a 98% yield of the reaction product when reducing 4-nitrophenol with hydrazine hydrate at 90 °C in ethanol–water for 1 h. Due to its strong paramagnetic properties (magnetization value of 55.9 emu g⁻¹), the catalyst was easily isolated and reused in at least 11 cycles without significant loss of activity or leaching. Also noteworthy is the biochemical application of the nanocomposite in an anticancer study of human lung adenocarcinoma cells against three cancer cell lines. The Fe_3O_4 /pectin/Au nanocomposite showed good antioxidant and antiradical properties, surpassing even the properties of the reference molecule, butylated hydroxytoluene. The nanocomposite also demonstrated significant cytotoxic activity against common human lung cancer cell lines, namely moderately differentiated lung adenocarcinoma (LC-2/ad), low-grade lung adenocarcinoma (PC-14) and well-differentiated bronchogenic lung adenocarcinoma (HLC-1), but unfortunately also against the normal HUVEC cell line. The best result with the lowest LC₅₀ values was achieved for PC-14 cell lines.

Hydrophilic catalysts based on Fe_3O_4 @ SiO_2 -T-G@Pd nanocomposites were developed and prepared by modifying magnetite first with tetraethyl orthosilicate (TEOS), then with 3-(trimethoxysilyl)-1-propanethiol (Figure 1, stage I), cyanuric chloride (Figure 1, stage II) and functionalization with glycerol (Figure 1, stage III), as well as *in situ* production of palladium nanoparticles on functionalized magnetite (Figure 1, stage IV).⁴

The Fe_3O_4 @ SiO_2 -T-G@Pd catalysts showed high activity in the sodium borohydride-mediated reduction of various nitroarenes, such as 4-nitrophenol, nitrobenzene, nitrotoluene,

as well as nitroarenes containing side amide functional groups and nitrobenzaldehydes. The analysis of vibration magnetometry data showed that the Fe_3O_4 @ SiO_2 and Fe_3O_4 @ SiO_2 -T-G@Pd nanocomposites, as well as the reused Fe_3O_4 @ SiO_2 -T-G@Pd retain superparamagnetic properties. The saturation magnetization values for Fe_3O_4 @ SiO_2 , Fe_3O_4 @ SiO_2 -T-G@Pd and recycled Fe_3O_4 @ SiO_2 -T-G@Pd reached 69, 53 and 52 emu g⁻¹, respectively, at zero residual magnetization and coercive force without a hysteresis loop, which proves their superparamagnetic properties and the possibility of extraction from the reaction medium. It turned out that the catalyst can be reused in seven cycles, which was demonstrated by the example of nitrobenzene reduction. It was also shown that the same catalyst exhibits high activity in the Suzuki–Miyaura cross-coupling reaction and in the one-step synthesis of paracetamol.⁴

High-purity reduced Fe_3O_4 (Red- Fe_3O_4) with 0.9% carbon content in the form of carboxylates and hydrocarbons was obtained from oil refining sludge and used as a catalyst for 4-nitrophenol reduction.⁶ Comparison of the properties of Red- Fe_3O_4 with a commercial sample of nano- Fe_3O_4 showed that Red- Fe_3O_4 exhibits higher efficiency with a complete conversion of 4-nitrophenol in 270 s, is easily isolated using a magnet, and is stable in five successive cycles without changing the activity. The activation energy was lower than that of commercial Fe_3O_4 . This study opens a new direction for using waste oil-containing sludge for catalyst preparation.

To catalyze the reduction reaction of 4-nitrophenol, Fe_3O_4 nanocrystals with three different morphologies (leaf-shaped, flower-shaped and flower-shaped spherical) were prepared using different amounts of urea (15, 90 and 270 mmol, respectively) and a probable growth mechanism was proposed.⁷ By controlling the addition of various amounts of Au particles, Fe_3O_4 –Au magnetic nanoparticles with different morphologies of Au nanoparticles were obtained. The structural and physical characteristics and catalytic activities of Fe_3O_4 –Au with different morphologies in the reduction reaction of rhodamine B and 4-nitrophenol were compared. A correlation was observed between the number of Au particles and the catalytic activity of Fe_3O_4 –Au magnetic nanoparticles. The reduction of 4-nitrophenol with sodium borohydride in the presence of flower-shaped Fe_3O_4 –Au nanoparticles resulted in the best

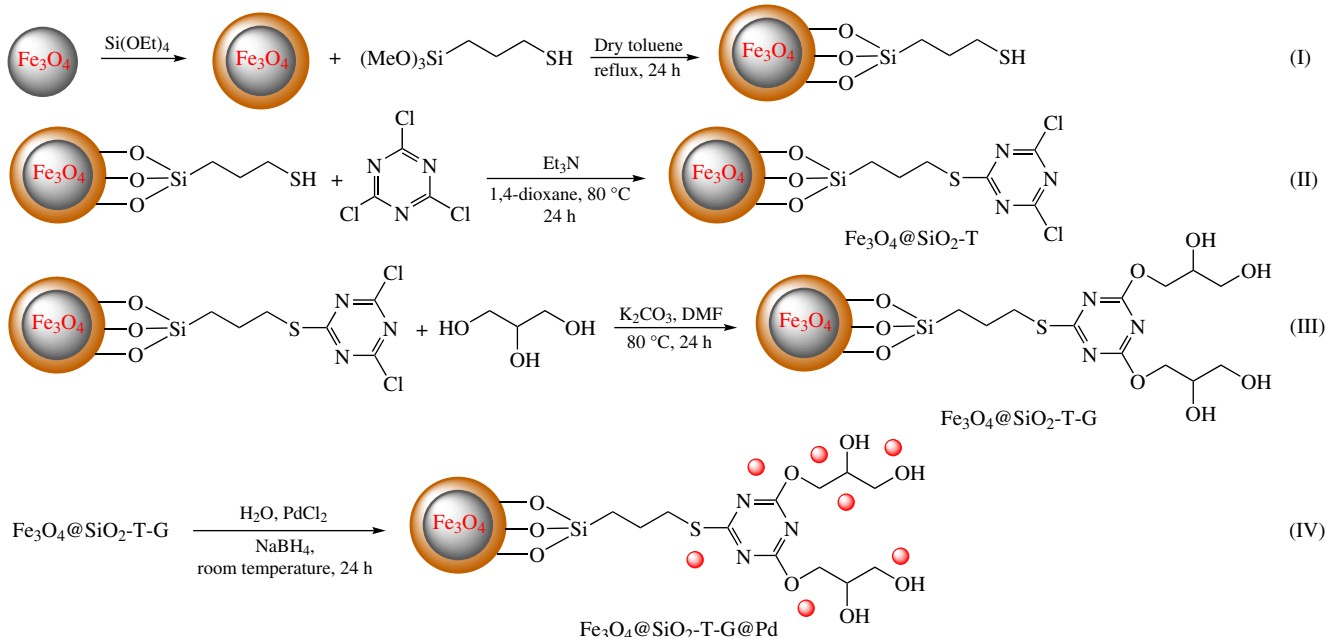


Figure 1 Preparation stages of Fe_3O_4 @ SiO_2 -T-G@Pd nanocomposites. Reproduced from ref. 4 with permission. Copyright 2023 Elsevier.

efficiency (96.7% yield) and followed pseudo-first-order kinetics. It was also found that the catalytic activity remained almost unchanged in six repeated cycles. The study sheds light on the effect of the morphology of high-performance and recyclable catalysts on the reduction of rhodamine B and 4-nitrophenol.

A group of researchers synthesized three-layer hollow hybrid h-Fe₃O₄@Au/polydopamine nanospheres by *in situ* redox polymerization. It was shown that due to the hollow core of h-Fe₃O₄, homogeneous functional polydopamine (PDA) coating and highly active Au nanocrystals, the h-Fe₃O₄@Au/PDA nanocomposite is capable of absorbing potentially toxic U^{VI} ions and catalyzing the reduction of 4-nitrophenol.^{8,9} In particular, it was found that due to the PDA coating, h-Fe₃O₄@Au/PDA remains stable in seven cycles, contributing to the conversion of 4-nitrophenol above 90%. It was also shown that h-Fe₃O₄@Au/PDA exhibits a good adsorption effect towards U^{VI} in nuclear waste, and its adsorption capacity reaches 82.9 mg g⁻¹ in six consecutive adsorption cycles. Magnetic h-Fe₃O₄@Au/PDA nanospheres were easily separated by applying an external magnetic field.¹¹

For the reduction of 4-nitrophenol with sodium borohydride, a Fe₃O₄@Alg-AuNPs nanocatalyst was prepared, consisting of Au nanoparticles decorating magnetite coated with sodium alginate.¹⁰ Sodium alginate, being a natural polysaccharide, acts as a stabilizing agent for the immobilization of Au nanoparticles. The reduction reaction was monitored using UV-VIS spectroscopy. It was found that in an aqueous medium at room temperature and a very low catalyst load (1–3 mg), the reaction proceeds in a short time (1.5–4 min) with a high yield (99%).

The catalyst was separated using a magnet and reused in eight cycles without loss of efficiency. Also, under mild conditions, the reaction of 4-nitrophenol reduction with sodium borohydride proceeded in the presence of a new catalyst based on gold nanoparticles supported on graphene oxide functionalized with chelate ligands. Thus, a high 97% conversion of 4-nitrophenol was achieved in 60 min.

Magnetic nanoparticles immobilized with poly(4-vinylpyridine) brushes were prepared by Cu⁰-mediated radical polymerization to coordinate Fe₃O₄@P4VP-Au nanoparticles (Figure 2).¹²

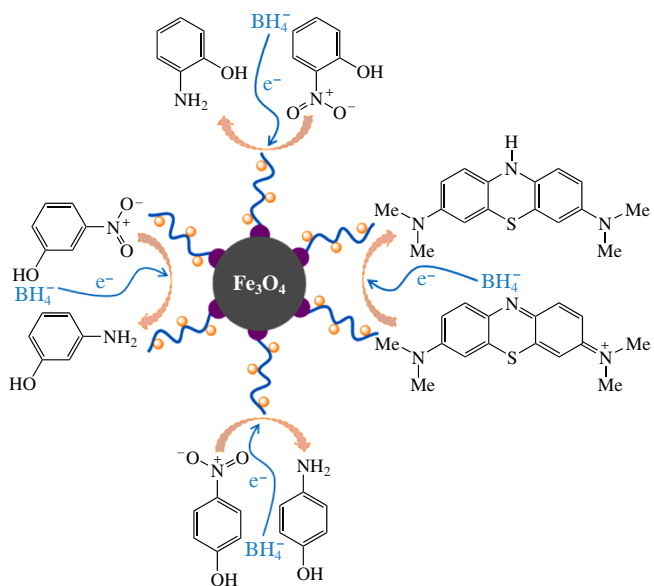


Figure 2 Mechanism of catalytic reduction of nitroaromatic compounds and methylene blue in the presence of Fe₃O₄@P4VP-Au. Reproduced from ref. 12 with permission. Copyright 2022 Elsevier.

The hybrid nanocatalyst Fe₃O₄@P4VP-Au was prepared in three stages. Initially, the initiator was obtained in the form of chlorinated Fe₃O₄-Cl by modifying the surface of commercial magnetite with 2-chloropropionyl chloride. In the second stage, as a result of radical polymerization of 4-vinylpyridine with reversible deactivation in the presence of Cu⁰ and tris[2-(dimethylamino)ethyl]amine, the formed brushes of polyvinylpyridine units were immobilized on the magnetite surface. And in the third stage, when hydrochloric acid was added to the Fe₃O₄@P4VP suspension in ethanol, Au was reduced and fixed *in situ* on the surface of polyvinylpyridine units. Thus, in this case, Fe₃O₄ and ethyl alcohol acted as reducing agents. And poly(4-vinylpyridine) served not only as a binder for Fe₃O₄ and Au nanoparticles but also as a stabilizer for 21.7 nm Au nanoparticles, preventing spontaneous aggregation. Fe₃O₄@P4VP-Au was effective in reducing 4-nitrophenol and methylene blue with TOF values of 12.3 and 0.7 min⁻¹, respectively. Since the catalyst was superparamagnetic (the saturation magnetization value was 40.2 emu g⁻¹, while the initial magnetite had a value of 56.7 emu g⁻¹) and therefore easily extracted from the reaction medium, the catalytic activity and morphology did not change significantly even after ten cycles.¹⁷

To immobilize ultrafine Au particles, a Fe₃O₄@COF core-shell support was prepared, in which the shell was a covalent organic framework (COF) with a magnetite core.¹³ Immobilization of gold nanoparticles in the framework channels was carried out by *in situ* reduction with sodium borohydride from a HAuCl₄ solution. The resulting Fe₃O₄@COF-Au sample exhibited high catalytic activity in the reduction of 4-nitrophenol and methylene blue with sodium borohydride. The catalyst demonstrated chemical stability and ease of magnetic separation from the reaction medium.

For the conversion of toxic impurities 4-nitrophenol and methylene blue in water, a catalyst Au/Fe₃O₄@MIL-100(Fe) based on metal-organic framework was prepared by the precipitation-reduction method,¹⁴ in which the magnetic core performs a dual function, both as a core and as a precursor of the Fe layer on the magnetite surface. It was shown that Au/Fe₃O₄@MIL-100(Fe) provides complete reduction of 4-nitrophenol and methylene blue in 16 min with high reaction rate constants *k* of 0.25 and 0.2 min⁻¹, respectively. In addition, Au/Fe₃O₄@MIL-100(Fe) was reused in five cycles without changing the catalytic activity.

Magnetic platinum catalysts based on the metal-organic framework Fe₃O₄@Pt@MIL-100(Fe) were synthesized by converting Fe₃O₄ into MIL-100(Fe) in a solution of benzene-1,3,5-tricarboxylic acid with encapsulation of platinum nanoparticles and subsequent adsorption on the magnetite surface during continuous growth of MIL-100(Fe) crystals.⁵ During the synthesis, a nanocomposite with a core-shell structure is formed. The catalytic activity of the nanocomposite was evaluated in the reaction of 4-nitrophenol reduction with sodium borohydride. It was shown that in the presence of Fe₃O₄@Pt@MIL-100(Fe) the reaction proceeds faster than in the presence of Fe₃O₄, Fe₃O₄@Pt and Fe₃O₄@MIL-100(Fe).

The synthesis of active heterometallic modified hollow Fe₃O₄ nanospheres (M-Fe₃O₄, M = Pd, Cu) is reported using a two-stage method involving solvothermal synthesis and calcination.¹⁵ Due to the uniformly distributed active heterometallic particles in the spherical shell of the hollow Fe₃O₄ nanospheres, the freshly prepared Pd-Fe₃O₄ catalyst exhibited high catalytic activity in the reduction of 4-nitrophenol with a TOF value of 145 min⁻¹, and also demonstrated excellent stability and magnetic regeneration ability. The catalytic efficiency of Pd-Fe₃O₄ is superior to most of the similar Fe₃O₄-supported metal catalysts reported in the literature. Interestingly, Cu-Fe₃O₄

exhibited five times higher activity in the oxidation of benzyl alcohol compared to pure Fe_3O_4 synthesized by the same method. Along with this, the conversion of 49.66% and the selectivity of 100% could be achieved. Moreover, the positive effect of Pd or Cu elements on the adsorption of 4-nitrophenol molecules was further confirmed by both experimental results and theoretical studies. The work demonstrates that enhancing the activity of iron oxides by modification with a heterometallic compound is a promising strategy for improving the catalyst performance.

A method for the production of silver nanoparticles embedded in magnetite functionalized with glutamic acid anion (Glu) was developed. Initially, magnetite nanoparticles were prepared by ion co-deposition in aqueous solutions followed by heat treatment.¹⁶ Then, magnetite was dispersed in water–methanol medium and its surface was coated with Glu ions. Finally, silver nanoparticles were synthesized by reduction of AgNO_3 with hydrazine hydrate and sodium borohydride. Fe_3O_4 -Glu-AgNPs nanoparticles were found to be an efficient reusable nanocatalyst with low catalyst loading in the reduction reaction of nitroarenes such as nitrophenol and nitroheteroarenes to the corresponding amines in the presence of NaBH_4 using water as an environmentally friendly solvent. The catalyst can be easily separated at the end of the reaction using an external magnet and reused for up to five cycles without any significant loss of catalytic activity. A study of the reduction of 4-nitrophenol on a larger scale showed that the catalyst can be recommended for industrial application.

To replace noble metal-based catalysts, an environmentally friendly $\text{Cu}_x\text{-FCLL}$ catalyst (where x denotes the number of mmol Cu) based on Cu/ Fe_3O_4 deposited on carbonized lotus leaves (CLL) obtained from agricultural waste was presented. The magnetic catalyst demonstrated high efficiency in the reduction of organic dyes (Congo red, methyl orange) and nitroaromatic compounds (3- and 4-nitrophenols).¹⁷ In the presence of Cu1.5-FCLL, the reduction of 4-nitrophenol with sodium borohydride was achieved in 30 s with a conversion rate of 98%, which is comparable with the widely used catalysts based on noble metals. It was shown that carbonized lotus leaves can be used to obtain an efficient carbon material with a unique tuberculate structure, which provides a large surface area, prevents the aggregation of metal nanoparticles and increases the catalytic activity of Cu1.5-FCLL due to the synergistic effect. The catalyst could be easily used with little loss of activity for at least 10 cycles.¹⁷

The Fe_3O_4 -cellulose–copper nanocomposite was synthesized by an environmentally friendly method using an aqueous extract of *Ceratonia siliqua* as a reducing and stabilizing agent.¹⁸ The catalytic activity of the synthesized catalyst was evaluated in the reduction of organic pollutants such as 4-nitrophenol, 2,4-dinitrophenylhydrazine, methyl orange and potassium ferricyanide in the presence of sodium borohydride (as a reducing agent) at room temperature. It was shown that this catalyst can also be used for the reduction of organic dyes and the selective oxidation of benzyl alcohol to benzaldehyde, providing high yields in a short reaction time.

Magnetic composite Cu-APTES@ Fe_3O_4 consisting of Cu clusters/atoms supported on (3-aminopropyl)triethoxysilane (APTES) functionalized magnetite was tested in the reduction of 4-nitrophenol.¹⁹ Spherical particles of the monodisperse composite up to 170 nm in size had a core–shell structure in which the core was Fe_3O_4 , and copper clusters (~8–10 nm) containing ~30–40 copper atoms were bound to the amino groups of APTES on the Fe_3O_4 surface. Almost complete reduction of 4-nitrophenol to 4-aminophenol was achieved within 10 min under the optimal reaction conditions: 25 °C,

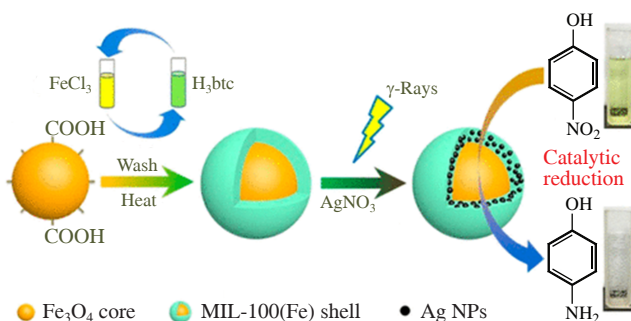


Figure 3 Preparation of Fe_3O_4 @MIL-100(Fe)/Ag-based nanocomposites. Reproduced from ref. 20 with permission. Copyright 2020 ACS.

0.17 mM 4-nitrophenol, 0.067 M NaBH_4 and 9.9 mg dm⁻³ Cu-APTES@ Fe_3O_4 .¹⁹

Magnetic nanocomposites Fe_3O_4 @MIL-100(Fe)/Ag decorated with silver nanoparticles were obtained by a simple method (Figure 3).²⁰ The nanocomposites had a structure of spherical particles with a Fe_3O_4 core with an average diameter of 400 nm, covered with a shell of a metal–organic framework MIL-100(Fe) with a thickness of 50 nm, with Ag nanoparticles uniformly distributed in their pores with a size of 2.0 ± 0.8 nm. Thus, due to the magnetic core, the nanocomposites had good magnetic properties and could be easily separated from the reaction medium, and the presence of Ag nanoparticles contributed to achieving high catalytic activity in the catalytic reduction of 4-nitrophenol.

If there was no Ag in the nanocomposite, the reaction did not occur within 60 min, *i.e.*, without silver, the Fe_3O_4 @MIL-100(Fe) nanocomposite does not exhibit catalytic activity.²⁰ Also in this work, the activities were compared with other MOF-based nanocomposites.

Using ultrasonic treatment and hydrothermal synthesis method, magnetite nanocomposite Ag/ Fe_3O_4 /CNC was prepared from silver nitrate and nanocrystalline cellulose (CNC), specially obtained from coconut husk, and used for the reduction of organic dyes.²¹ In this case, the cellulose matrix served as a reducing agent for silver ions and a stabilizer for the newly formed nanoparticles. The composite made it possible to rapidly reduce and decolorize aqueous solutions with sodium borohydride in a short time (2 to 5 min) using small amounts of a catalyst ranging from 2.5 mg for 4-nitrophenol to 15 mg for methyl orange and methylene blue in water at 25 °C. Hydrolysis of sodium borohydride in aqueous solution leads to the formation of hydrogen, electron-rich hydrogen-mediator complexes (silver hydride) and an electron relay-type system for the reduction of organic compounds. The magnetic catalyst was removed and reused three times without reducing the catalytic activity. The work is essential for reducing the amounts of harmful organic pollutants in wastewater for environmental protection.²¹

Following a simple synthesis strategy, bifunctional Fe_3O_4 @C– MoO_2 –Ni composites were prepared, which were found to be effective reusable catalysts for the reduction of 4-nitrophenol to 4-aminophenol.²² Initially, magnetite particles were obtained by a solvothermal method, which were subsequently coated with a resorcinol-formaldehyde polymer shell by polymerizing resorcinol-formaldehyde on their surface. Then, the resorcinol-formaldehyde shell was impregnated with nickel chloride, urea and sodium molybdate solutions and subjected to subsequent carbonization without using an additional reducing agent to form core–shell Fe_3O_4 @C particles containing dispersed high-density Ni particles. The carbon coating layer on the Fe_3O_4 magnetic spheres protected the Fe_3O_4 particles from oxidation and acid exposure and also acted as a carrier. The Fe_3O_4 @C– MoO_2 –Ni based composites demonstrated

high catalytic efficiency in the reduction of 4-nitrophenol to 4-aminophenol ($k = 0.01465 \text{ s}^{-1}$), significantly exceeding the efficiency of previously known catalysts. In addition, the $\text{Fe}_3\text{O}_4@\text{C-MoO}_2\text{-Ni}$ composites had outstanding magnetic properties (saturation magnetization of 40.34 emu g^{-1}), which ensured their suitability for reuse by magnetic separation from solution. The $\text{Fe}_3\text{O}_4@\text{C-MoO}_2\text{-Ni}$ composites also demonstrated fast adsorption rate and high adsorption capacity (88.95 mg g^{-1}) for methylene blue. Due to these adsorption properties, the $\text{Fe}_3\text{O}_4@\text{C-MoO}_2\text{-Ni}$ system is an ideal adsorbent for the removal of methylene blue from water.²²

A $\text{Fe}_3\text{O}_4\text{-SiO}_2\text{-Cu}_2\text{O/Cu}$ nanomaterial with a magnetic core-shell structure was synthesized using Fe_3O_4 as a magnetic core for ease separation of the catalyst from the reaction medium and SiO_2 as a binding layer, with Cu particles uniformly distributed over the surface of the $\text{Fe}_3\text{O}_4\text{-SiO}_2\text{-Cu}_2\text{O/Cu}$ nanostructure.²³ The nanomaterial was used as an effective catalyst for the reduction of 4-nitrophenol with sodium borohydride, where the conversion of 4-nitrophenol reached 100% within 5 min. Moreover, the $\text{Fe}_3\text{O}_4\text{-SiO}_2\text{-Cu}_2\text{O/Cu}$ composite is recyclable, retaining a catalytic activity of more than 90% even after 24 catalysis cycles.

The cited work²⁴ demonstrated the use of agricultural waste from corn processing in the reaction of catalytic reduction of 4-nitrophenol with sodium borohydride. For this purpose, magnetite-modified corn straw was prepared by amidation reaction of succinylated corn straw (S-MS) with amino-functionalized magnetite nanoparticles ($\text{NH}_2\text{-Fe}_3\text{O}_4$) and used as a support for the catalyst based on Cu and Cu_2O nanoparticles. After mixing magnetic succinylated corn straw (Mag-S-MS) with an aqueous solution of copper ion salts, Cu^{2+} is captured by amino and carboxylate groups and reduced by sodium borohydride (NaBH_4). It was shown that binary $\text{Cu/Cu}_2\text{O}$ nanocomposites were successfully formed on Mag-S-MS without self-aggregation and oxidation. SEM-EMF images showed that $\text{Cu/Cu}_2\text{O}$ particles having a flower-like structure were uniformly distributed on the surface of Mag-S-MS and had a diameter of 220–800 nm. Cu and Cu_2O nanoparticles play a synergistic role in the conversion of hydrogen and electrons, thereby increasing the catalytic efficiency compared with other known catalysts. Mag-S-MS containing $\text{Cu/Cu}_2\text{O}$ had high catalytic efficiency in the reduction of 4-nitrophenol to

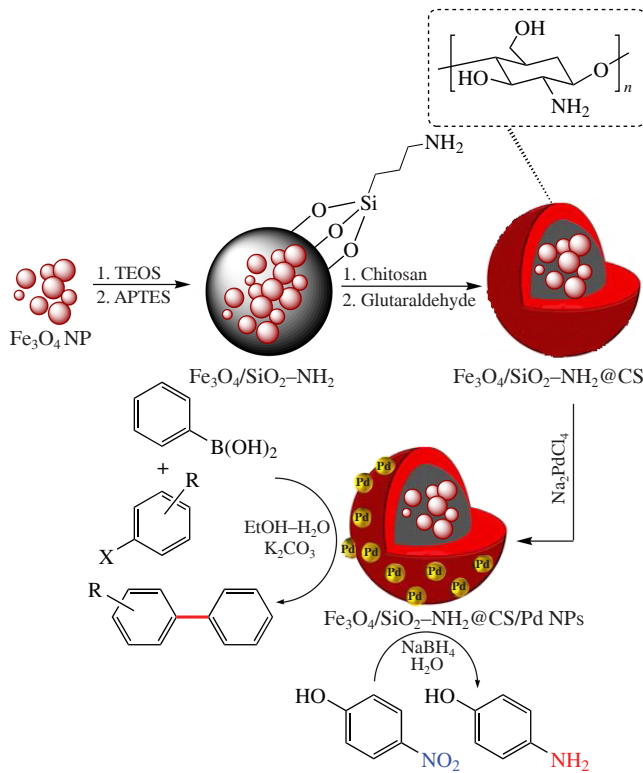


Figure 4 Preparation of $\text{Fe}_3\text{O}_4\text{/SiO}_2\text{-NH}_2\text{@CS/Pd}$ nanocomposite and its application in the Suzuki coupling and 4-nitrophenol reduction reactions. Reproduced from ref. 26 with permission. Copyright 2020 Elsevier.

4-aminophenol. The kinetics of the reduction process corresponded to a pseudo-first-order reaction. Increasing the amount of catalyst and NaBH_4 accelerated the reduction reaction, while increasing the concentration of 4-nitrophenol had the opposite effect. Due to its superparamagnetism, the catalyst was easily separated from the solution under the influence of an external magnetic field. Repeated cycle testing of the catalyst showed that the catalytic activity did not decrease significantly after five cycles.

An efficient catalyst for the reduction of 4-nitrophenol to 4-aminophenol as well as for the Suzuki coupling reaction was prepared starting from magnetite nanoparticles supported on

Table 1 Comparison of TOF of various magnetite supported catalysts in the hydrogenation reaction of 4-nitrophenol with sodium borohydride in water.

| Entry | Source | Catalyst | Time/min | Active metal content (wt%) | TOF/min ⁻¹ | Number of cycles |
|-------|---------|---|----------|----------------------------|-----------------------------------|------------------|
| 1 | Ref. 16 | Red- Fe_3O_4 | 4.5 | – | – | 5 |
| 2 | Ref. 7 | $\text{Fe}_3\text{O}_4\text{-Au FA20}$ | 9 | – | 9.58 | 6 |
| 3 | Ref. 13 | $\text{Fe}_3\text{O}_4@\text{COF-Au}$ | 24 | – | 5.91 | 5 |
| 4 | Ref. 8 | h- $\text{Fe}_3\text{O}_4@\text{Au/PDA}$ | 4.5 | 12.8 | 1.0 ^a | 7 |
| 5 | Ref. 18 | $\text{Fe}_3\text{O}_4\text{-C-Cu}^b$ | 3.2 | 13.37 | – | 4 |
| 6 | Ref. 10 | $\text{Fe}_3\text{O}_4@\text{Alg-AuNPs}^c$ | 1.5 | 3.6 | – | 8 |
| 7 | Ref. 28 | $\text{Fe}_3\text{O}_4\text{/SiO}_2\text{-NH}_2\text{@CS/Pd NPs}$ | 4 | 1.62 | 1.2×10^{-2} ^d | 8 |
| 8 | Ref. 15 | $\text{Pd-Fe}_3\text{O}_4$ | – | – | 145 | – |
| 9 | Ref. 15 | $\text{Cu-Fe}_3\text{O}_4$ | 0.7–0.8 | – | 7.3 | – |
| 10 | Ref. 19 | $\text{Cu-APTES}@{\text{Fe}_3\text{O}_4}$ | 10 | – | 100 ^e | 9 |
| 11 | Ref. 25 | $\text{Co-Fe}_3\text{O}_4@\text{C-A}^f$ | 0.833 | 3.88 | 3.43 | 5 |
| 12 | Ref. 24 | $\text{Ni-Fe}_3\text{O}_4@\text{C-A}$ | 1.33 | 12.75 | 1.66 | – |
| 13 | Ref. 24 | $\text{Ag}@{\text{Fe}_3\text{O}_4}$ | 8 | – | – | 5 |
| 14 | Ref. 21 | $\text{Ag/Fe}_3\text{O}_4/\text{CNC}^g$ | 10 | 13.89 | – | 3 |
| 15 | Ref. 20 | $\text{Fe}_3\text{O}_4@\text{MIL-100(Fe)}/\text{Ag}$ | – | – | 19.93 | – |
| 16 | Ref. 20 | $\text{Fe}_3\text{O}_4@\text{MIL-100(Fe)}/\text{Ag}$ | 1 | – | 42.75 | 5 |
| 17 | Ref. 26 | $\text{Fe}_3\text{O}_4@\text{SiO}_2\text{-T-G@Pd}$ | 15 | 0.1 ^h | 66 | – |
| 18 | Ref. 22 | $\text{Fe}_3\text{O}_4@\text{Pt}@{\text{MIL-100(Fe)}}$ | 7 | 2.15 | 19.93 | – |
| 19 | Ref. 17 | $\text{Fe}_3\text{O}_4@\text{P4VP-Au}$ | 60 | – | 12.33 | – |

^aRate constant k . ^b Fe_3O_4 -cellulose-Cu. Found (%): Cu, 13.37; Fe, 34.49. ^cAu NPs decorating alginate-coated magnetite. ^dRate constant k (s^{-1}). ^eConversion (%). ^fMagnetite inside a porous carbon shell decorated with Co. ^gNanocellulose with magnetite and Ag NPs. ^hMol% Pd.

mesoporous silica microparticles, which in turn were functionalized by TEOS and APTES to introduce terminal amino groups and embedded in a chitosan matrix.²⁶ The catalyst was further modified with palladium to create active sites for the Suzuki cross-coupling reaction and the reduction of 4-nitrophenol to the corresponding amine in high yields of the target products (Figure 4).

Fe_3O_4 prepared *ex situ* by the solvothermal method was modified with the silane coupling agent KH570. A copolymer of divinylbenzene (DVB) and glycidyl methacrylate (GMA) was synthesized by the distillation precipitation polymerization to coat the magnetite core, which was then functionalized with

amino groups in the presence of 1,6-hexanediamine. Using Michael addition and amidation reactions, poly(amidoamine) dendrimers were grafted onto the $\text{Fe}_3\text{O}_4/\text{P}(\text{GMA}-\text{DVB})$ surface, whereby the active groups of the poly(amidoamine) tree became the binding sites and carriers for gold nanoparticles formed after the addition of hydrochloric acid to the resulting microspheres by the reduction of Au^{3+} to Au^0 with sodium borohydride.²⁷ It was shown that in the obtained $\text{Fe}_3\text{O}_4/\text{P}(\text{GMA}-\text{DVB})/\text{PAMAM}/\text{Au}$ nanocomposites, the magnetite core reaches 170 nm. The translucent polymer shell has a thickness of more than 80 nm, and the Au nanoparticles are 7–10 nm in size (Figure 5). High conversion was achieved

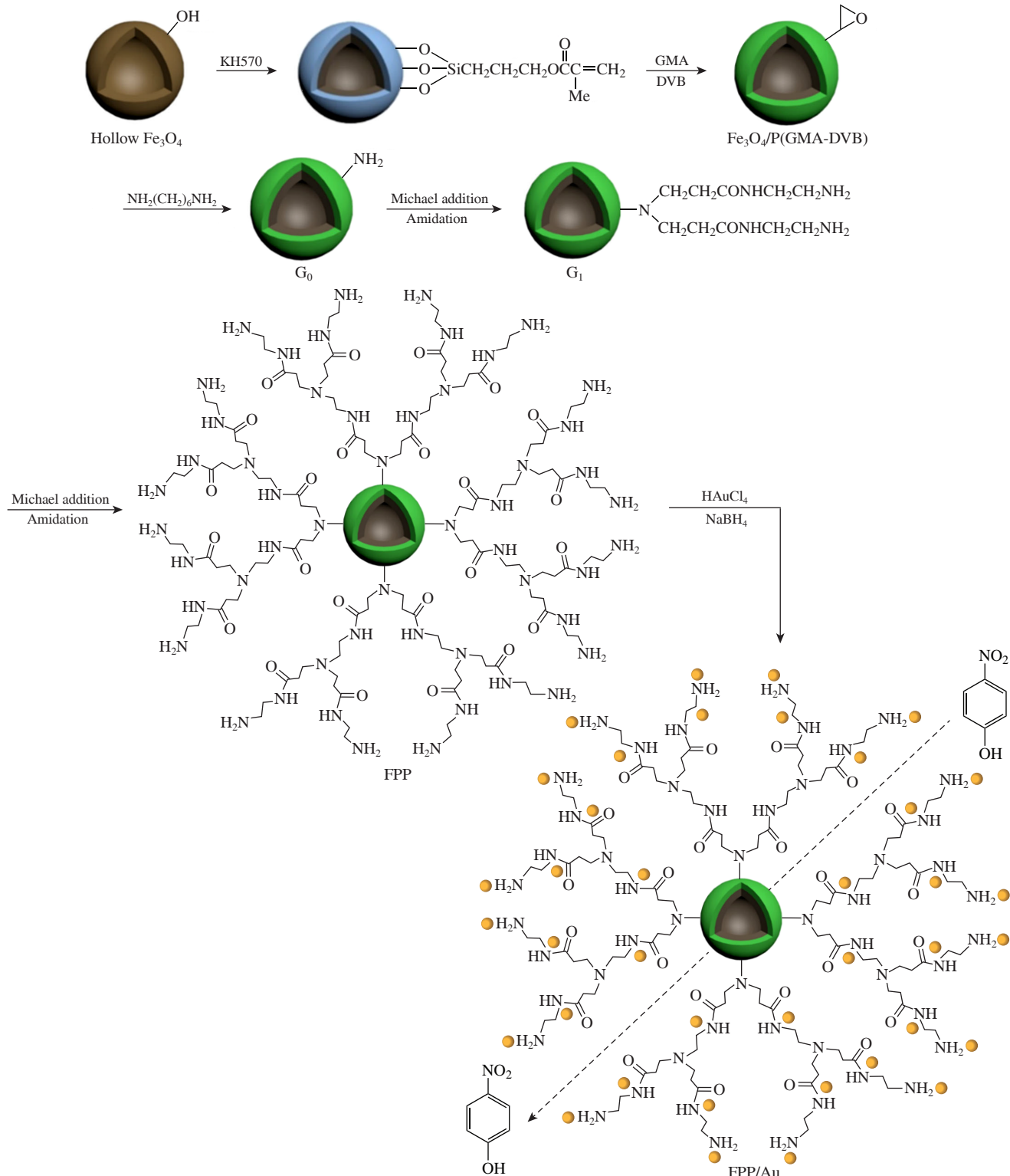


Figure 5 Preparation of $\text{Fe}_3\text{O}_4/\text{P}(\text{GMA}-\text{DVB})/\text{PAMAM}/\text{Au}$ (FPP/Au) nanospheres. Reproduced from ref. 27 with permission. Copyright 2019 Elsevier.

in 7 min at 45 °C in the presence of $\text{Fe}_3\text{O}_4/\text{P}(\text{GMA}-\text{DVB})/\text{PAMAM}/\text{Au}$ suspension with a concentration of 1 g dm⁻³. The nanoparticles were stable in 10 cycles, easily separated from the reaction medium and reused.

Table 1 summarizes the data for various magnetite supported catalysts to compare the TOF in the hydrogenation reaction of 4-nitrophenol with sodium borohydride in water.

Reduction of furfural

The furfural reduction reaction is currently attracting attention as an approach to convert platform chemicals into value-added products (Scheme 3).



Scheme 3 Hydrogenation of furfural to furfuryl alcohol.

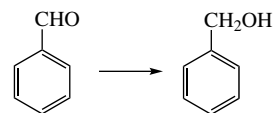
Magnetic nanoparticles Fe_3O_4 -12 with a particle size of 12 nm, used as an easily separable heterogeneous catalysts, exhibited high activity in the reaction of catalytic hydrogenation of furfural to furfuryl alcohol with hydrogen transfer from isopropanol as a hydrogen source, while the yield of furfuryl alcohol was 90.1% at 160 °C for 5 h.²⁸

Comparison of Fe_3O_4 nanoparticles of different sizes showed that the smaller the nanoparticles, the smaller the pore diameter and the larger the surface area of the material. This leads to the appearance of acid–base active centers and relatively low activation energy. In addition, the reduction experiment involving the dehydration of xylose to furfural and then the reduction of furfural to furfuryl alcohol confirmed that the catalytic system has great potential for industrial application. A possible flowchart of the chemical process from xylose to furfuryl alcohol was developed, which can realize the transformation of biomass resources (e.g., xylose obtained from corn cobs) into various valuable organic compounds with the reuse of catalysts and solvents, and minimize the amount of solvents and pollutant emissions.

In order to efficiently hydrogenate furfural into furfuryl alcohol with molecular hydrogen, magnetically separable catalysts containing Pd^0 or Pt^0 particles with a diameter of ~3 nm and magnetic nanoparticles stabilized with polyphenylquinoxaline (PFX) or hyperbranched pyridylphenylene polymer (SRPFP) were prepared.²⁹ The maximum selectivity was achieved at 120 °C and a hydrogen pressure of 6 MPa using isopropanol as a solvent. It was shown that isopropanol is exactly the solvent of medium polarity in which a balance is achieved between the solubility of furfuryl alcohol and its acceptable access to catalytic centers, which ensures the highest catalyst activity and process selectivity. A comparison of the catalytic activity of Pd-containing magnetite nanoparticles stabilized by PFX (Pd-PFX) and SRPFP (Pd-SRPFP) was performed, which showed the advantages of the hyperbranched structure of SRPFP compared to the linear structure of PFX. Thus, in the presence of Pd-SRPFP, high selectivity of furfuryl alcohol formation (99.3%) was achieved at a conversion of 99.8%, high activity (871 min⁻¹) and stability. This effect of Pd-SRPFP was explained by the following reasons: (1) the structure of the catalyst, in which Pd nanoparticles are separated from magnetite nanoparticles due to the branched structure of SRPFP; (2) shielding of magnetite particles with SRPFP, which minimizes the effect of magnetite on the conversion of furfural to isopropyl furfuryl ether, thereby contributing to higher selectivity for furfuryl alcohol.

Hydrogenation of benzaldehyde

Hydrogenation of benzaldehyde (Scheme 4) can be considered as a model reaction for the hydrogenation of oxo compounds (aldehydes and ketones).

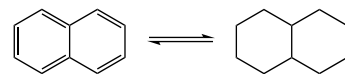


Scheme 4 Hydrogenation of benzaldehyde to benzyl alcohol.

A number of stable noble metal-free $\text{Ni}/\text{Fe}_3\text{O}_4$ -based magnetic catalysts were prepared from double layered NiFe hydroxides by a simple calcination–reduction method.³³ The catalysts with a $\text{Ni}^{2+}/\text{Fe}^{3+}$ ratio of 1 were effective in the selective hydrogenation of benzaldehyde to chemically pure benzyl alcohol and in the hydrogenation of furfural to the biofuel 2-methylfuran with high yields (99.0 and 78.4%, respectively) under mild conditions. Systematic studies have shown that the $\text{Ni}^{2+}/\text{Fe}^{3+}$ ratio affects the dispersion and surface acidity of the catalysts, which play a crucial role in achieving the efficiency of the catalytic reaction. As an example, the effects of solvent and reaction parameters, as well as the possibility of reusing the catalysts in the benzaldehyde hydrogenation process, were studied. It was shown that the strong interaction between Ni and Fe_3O_4 particles increases the stability of the catalyst. The mechanism of the catalytic reaction of selective hydrogenation of furfural to 2-methylfuran was discussed. Thus, the work demonstrated the possibility of using a catalyst that does not contain a noble metal for the selective hydrogenation of chemicals obtained from biomass.³⁴

Hydrogenation of naphthalene

Recently, the hydrogenation of naphthalene has gained importance in the field of hydrogen storage, with the naphthalene–decalin pair (Scheme 5) being considered as a benign alternative to light hydrocarbons.



Scheme 5 Reversible hydrogenation–dehydrogenation processes in the naphthalene–decalin pair.

A magnetically separable silica-supported palladium catalyst was developed and prepared for the selective hydrogenation of naphthalene to tetralin.³⁴ In the catalyst, Pd nanoparticles were evenly distributed and protected by mesoporous silica shells deposited on the Fe_3O_4 cores, thus significantly improving the stability of the catalyst. Repeated use of this catalyst in naphthalene hydrogenation resulted in complete conversion and production of 77 to 90% of tetralin.

Hydrogenation of carbon dioxide

Hydrogenation of carbon dioxide is a hot topic nowadays, since it allows partial utilization of this greenhouse gas by converting it into CO, hydrocarbons, methanol and other valuable products. A number of catalysts based on rubidium-promoted Fe_3O_4 microspheres have been developed for the catalytic reaction of carbon dioxide hydrogenation to light olefins.³⁵ Although magnetic separation was not used in the catalytic process, it could be effectively used at the stage of separating the finished catalyst from the mixture used for its preparation. The 3 wt% $\text{Rb}/\text{Fe}_3\text{O}_4$ catalyst showed high selectivity of 47.4% for the formation of light C₂–C₄ olefins with a high olefin to paraffin ratio of 10.7. Table 2 shows the activity and selectivity of magnetite-based catalysts depending on the rubidium content.

Studies using temperature-programmed hydrogen reduction, temperature-programmed desorption and X-ray photoelectron spectroscopy showed that a certain Rb content could control the carbonaceous particles content and iron oxide content on the

Table 2 Activity and selectivity of magnetite-based catalysts with different Rb content in carbon dioxide hydrogenation.³⁶

| Entry | Catalyst | CO ₂ conversion ^a (%) | Selectivity (%) | | Selectivity to hydrocarbons (mol%) | | | Olefin/paraffin (C ₂ –C ₄) ^b | |
|-------|--------------------------------------|---|-----------------|------|------------------------------------|--------------------------------|-----------------|--|------|
| | | | CO | ROH | C ₁ | C ₂ –C ₄ | C ₅₊ | | |
| 1 | Fe ₃ O ₄ | 37.2 | 7.3 | 0 | 44.9 | 27.1 | 16.0 | 12.0 | 1.7 |
| 2 | 1% Rb/Fe ₃ O ₄ | 40.8 | 6.0 | 5.4 | 30.8 | 37.1 | 5.9 | 26.2 | 6.3 |
| 3 | 3% Rb/Fe ₃ O ₄ | 39.7 | 8.1 | 14.7 | 19.5 | 47.4 | 4.4 | 28.7 | 10.7 |
| 4 | 5% Rb/Fe ₃ O ₄ | 38.3 | 6.9 | 13.7 | 18.2 | 41.8 | 3.8 | 36.2 | 11.0 |
| 5 | 8% Rb/Fe ₃ O ₄ | 38.2 | 7.3 | 13.6 | 17.9 | 39.8 | 3.4 | 38.9 | 11.7 |

^aReaction conditions: 300 °C, 0.5 MPa, H₂/CO₂ = 1:3, GHSV = 2500 cm³ g_{cat}⁻¹ h⁻¹. ^bOlefin/paraffin molar ratio in C₂–C₄ mixture.

catalyst surface, which contributed to the synergistic effect in the production of light olefins.

The Fe₃O₄/BN and Fe₃O₄(Pt)/BN nanoheterostructures were obtained by the polyol method, in which hexagonal boron nitride was used as a carrier of Fe₃O₄ nanoparticles.³⁶ The resulting materials were used in the process of CO₂ hydrogenation. It was shown that Fe₃O₄/BN and Fe₃O₄(Pt)/BN are selective with respect to hydrocarbons.

The catalyst based on Ru–Fe₃O₄/CeO_x–SiO₂ (Ce³⁺/Ce⁴⁺, x = 1.64) synthesized by impregnation of Ru and Fe₃O₄ nanoparticles on cerium-promoted mesoporous silica support SBA-15 turned out to be effective in selective reduction of CO₂ to methane.³⁷ Thus, the conversion of CO₂ reached 82% with a ruthenium content of 0.25 wt% and a Fe₃O₄ content of 2.5 wt% at a temperature of 575 K, a pressure of 20 bar, a gas hourly space velocity (GHSV) of 3000 cm³ g⁻¹ h⁻¹ and an H₂/CO molar ratio of 5:1 in a fixed-bed reactor. Close contact between ruthenium and magnetite nanoparticles contributed to the reduction of CO₂ through the effect of hydrogen spillover, and cerium oxide nanoparticles were the promoters of this reduction reaction. Density functional theory studies showed that the large surface area and large mesopores of the silica support promote fine dispersion of active catalytic centers and oxygen vacancies.

Oxygen reduction reaction

Fe₃O₄ nanoparticles embedded in atomically dispersed Fe–N–C catalyst, in which iron atoms are coordinated to nitrogen-doped carbon support, were used in an efficient oxygen reduction reaction (ORR) to establish the effect of micro- and macropores.³⁸ Atomically dispersed Fe–N–C catalysts encapsulated with magnetite nanoparticles demonstrate great potential for catalysis of ORR.³⁵ Fe₃O₄ nanoparticles encapsulated in atomically dispersed Fe–N–C electrochemical catalyst were synthesized by high-temperature pyrolysis of polyacrylonitrile and FeCl₃. The effect of micro- and macropores in the catalysts prepared and controlled by the addition of SiO₂ and ZnCl₂ templates on the structure and electrochemical properties was studied. It was shown that the presence of micropores favors the nucleation and retention of Fe₃O₄ nanoparticles. On the other hand, the macropores contribute to a lower Fe₃O₄ content, a higher nitrogen content and current density limitation. The optimized Fe₃O₄@FeNC catalyst with micro- and macropores showed ORR activity comparable to that of the known catalysts and superior to that of commercial Pt/C, suggesting its potential application in real devices. More importantly, the porous architecture not only affects the mass transport and active centers, but also has a huge impact on the nucleation of Fe₃O₄ nanoparticles, the graphitization degree of the carbon support, the chemical environment of the elements and the catalytic pathways of ORR. Density functional theory calculations show stronger adsorption of O₂ on Fe–N–C when it is deposited on Fe₃O₄ fragments, which can increase the reactant concentration for ORR and enhance the overall activity. These results provide important guidance for the future understanding and development of single-atom catalysts with improved electrochemical properties.

Conclusion

Thus, the research was particularly focused on the development of separable magnetic nanocatalysts due to the possibility of their easy separation and isolation from the reaction medium. In order to increase the stability of magnetite nanoparticles, they are embedded in various matrices. Therefore, much attention is paid to nanostructured and composite materials with a core–shell structure, in which the core is magnetite, and the shell can be of both organic (polymer, biopolymer) and inorganic (silicon dioxide, graphene oxide) nature. In reduction reactions, most of the considered magnetic catalysts are characterized by high activity, stability and the possibility of reuse in several cycles without a significant decrease in activity.

This work was financially supported by the Ministry of Science and Higher Education of the Russian Federation (grant no. 075-15-2023-585). This work was conducted within the framework of the ISMAN State Assignment.

References

- 1 A. Yu. Olenin and G. V. Lisichkin, *Russ. J. Gen. Chem.*, 2019, **89**, 1451; <https://doi.org/10.1134/S1070363219070168>.
- 2 L. Zhao, K. Zheng, J. Tong, J. Jin and C. Shen, *Catal. Lett.*, 2019, **149**, 2607; <https://doi.org/10.1007/s10562-019-02829-0>.
- 3 Y. Li, N. Li, W. Jiang, G. Ma and M. M. Zangeneh, *Int. J. Biol. Macromol.*, 2020, **163**, 2162; <https://doi.org/10.1016/j.ijbiomac.2020.09.102>.
- 4 M. Gholinejad, H. Bagheri, F. Zareh and J. M. Sansano, *J. Mol. Struct.*, 2023, **1288**, 135804; <https://doi.org/10.1016/j.molstruc.2023.135804>.
- 5 X. Chen, Y. Zhang, Y. Zhao, S. Wang, L. Liu, W. Xu, Z. Guo, S. Wang, Y. Liu and J. Zhang, *Inorg. Chem.*, 2019, **58**, 12433; <https://doi.org/10.1021/acs.inorgchem.9b02114>.
- 6 W. Xia, F. Zhao, P. Fang, M. An, J. Zhu, K. Cheng and M. Xia, *Sep. Purif. Technol.*, 2023, **309**, 123018; <https://doi.org/10.1016/j.seppur.2022.123018>.
- 7 Y. Kou, T. Wu, G. Xing, X. Huang, D. Han, S. Yang, C. Guo, W. Gao, J. Yang, Y. Liu and D. Wang, *Nanotechnology*, 2020, **31**, 225701; <https://doi.org/10.1088/1361-6528/ab767b>.
- 8 K. Xu, J. Wu, Q. Fang, L. Bai, J. Duan, J. Li, H. Xu, A. Hui, L. Hao and S. Xuan, *Chem. Eng. J.*, 2020, **398**, 125571; <https://doi.org/10.1016/j.cej.2020.125571>.
- 9 Q. Fang, J. Zhang, L. Bai, J. Duan, H. Xu, K. C.-F. Leung and S. Xuan, *J. Hazard. Mater.*, 2019, **367**, 15; <https://doi.org/10.1016/j.jhazmat.2018.12.059>.
- 10 R. Ghorbani-Vaghei, H. Veisi, M. H. Aliani, P. Mohammadi and B. Karmakar, *J. Mol. Liq.*, 2021, **327**, 114868; <https://doi.org/10.1016/j.molliq.2020.114868>.
- 11 F. M. Moghaddam, A. Siahpoosh and M. Eslami, *J. Iran. Chem. Soc.*, 2023, **20**, 381; <https://doi.org/10.1007/s13738-022-02673-x>.
- 12 M. Hong, X. Xu, B. Wang, Z. Guan, Z. Zheng and Q. Zhang, *Colloids Surf. A*, 2022, **639**, 128338; <https://doi.org/10.1016/j.colsurfa.2022.128338>.
- 13 Y. Xu, X. Shi, R. Hua, R. Zhang, Y. Yao, B. Zhao, T. Liu, J. Zheng and G. Lu, *Appl. Catal. B*, 2020, **260**, 118142; <https://doi.org/10.1016/j.apcatb.2019.118142>.
- 14 S. Aslam, F. Subhan, Z. Liu, Z. Yan, A. Ahmad, A. Nazir, A. Siddiqi and M. Yaseen, *Colloids Surf. A*, 2023, **660**, 130904; <https://doi.org/10.1016/j.colsurfa.2022.130904>.
- 15 L. Wen, D. Wang, J. Xi, F. Tian, P. Liu and Z.-W. Bai, *J. Catal.*, 2022, **413**, 779; <https://doi.org/10.1016/j.jcat.2022.07.036>.

16 M. Kumari, R. Gupta and Y. Jain, *Appl. Organomet. Chem.*, 2019, **33**, e5223; <https://doi.org/10.1002/aoc.5223>.

17 X. Huang, C. Lin, X. Ding, Y. Yang and H. Ge, *Mater. Sci. Eng., B*, 2023, **293**, 116465; <https://doi.org/10.1016/j.mseb.2023.116465>.

18 E. Kalantari, M. A. Khalilzadeh, D. Zareyee and M. Shokouhimehr, *J. Mol. Struct.*, 2020, **1218**, 128488; <https://doi.org/10.1016/j.molstruc.2020.128488>.

19 Y. Zhong, Y. Gu, L. Yu, G. Cheng, X. Yang, M. Sun and B. He, *Colloids Surf., A*, 2018, **547**, 28; <https://doi.org/10.1016/j.colsurfa.2018.03.015>.

20 S. Chang, C. Liu, Y. Sun, Z. Yan, X. Zhang, X. Hu and H. Zhang, *ACS Appl. Nano Mater.*, 2020, **3**, 2302; <https://doi.org/10.1021/acsanm.9b02415>.

21 A. N. Vu, H. N. T. Le, T. B. Phan and H. V. Le, *Polymers*, 2023, **15**, 3373; <https://doi.org/10.3390/polym15163373>.

22 L. Zhang, X. Liu, M. Zhang, H. Yuan, L. Zhang and J. Lu, *Appl. Surf. Sci.*, 2019, **494**, 783; <https://doi.org/10.1016/j.apsusc.2019.07.249>.

23 S. Sun, Z. Zhang, S. Li, J. Le, H. Qian, X. Yin, Y. Liu, W. Yang and Y. Chen, *J. Mater. Sci.*, 2023, **58**, 5587; <https://doi.org/10.1007/s10853-023-08377-8>.

24 Y. Yu, H. Guo, P. Wang, S. Zhai, J. Han, W. Li, Y. Wang and Y. Wang, *Res. Chem. Intermed.*, 2023, **49**, 381; <https://doi.org/10.1007/s11164-022-04889-1>.

25 A. E. Baye, R. Appiah-Ntiamoah and H. Kim, *Sci. Total Environ.*, 2020, **712**, 135492; <https://doi.org/10.1016/j.scitotenv.2019.135492>.

26 H. Veisi, T. Ozturk, B. Karmakar, T. Tamoradi and S. Hemmati, *Carbohydr. Polym.*, 2020, **235**, 115966; <https://doi.org/10.1016/j.carbpol.2020.115966>.

27 M. Ma, Y. Yang, W. Li, R. Feng, Z. Li, P. Lyu and Y. Ma, *J. Mater. Sci.*, 2019, **54**, 323; <https://doi.org/10.1007/s10853-018-2868-1>.

28 M. Ma, P. Hou, P. Zhang, J. Cao, H. Liu, H. Yue, G. Tian and S. Feng, *Appl. Catal., A*, 2020, **602**, 117709; <https://doi.org/10.1016/j.apcata.2020.117709>.

29 K. Alibegovic, D. G. Morgan, Y. Losovyj, M. Pink, B. D. Stein, N. V. Kuchkina, E. S. Serkova, K. E. Salnikova, Z. B. Shifrina, V. G. Matveeva, E. M. Sulman and L. M. Bronstein, *ChemistrySelect*, 2017, **2**, 5485; <https://doi.org/10.1002/slct.201701100>.

30 D. V. Pryazhnikov, O. O. Efanova and I. V. Kubrakova, *Mendeleev Commun.*, 2024, **34**, 427; <https://doi.org/10.1016/j.mencom.2024.04.037>.

31 Y. Zhou and L. Wang, *Mendeleev Commun.*, 2023, **33**, 699; <https://doi.org/10.1016/j.mencom.2023.09.034>.

32 I. I. Mishanin, T. V. Bogdan, A. V. Smirnov, P. A. Chernavskii, N. N. Kuznetsova and V. I. Bogdan, *Mendeleev Commun.*, 2023, **33**, 422; <https://doi.org/10.1016/j.mencom.2023.04.039>.

33 Y. Wang, D. Hu, R. Guo, H. Deng, M. Amer, Z. Zhao, H. Xu and K. Yan, *Mol. Catal.*, 2022, **528**, 112505; <https://doi.org/10.1016/j.mcat.2022.112505>.

34 Y. Yang, B. Xu, J. He, J. Shi, L. Yu and Y. Fan, *Appl. Organomet. Chem.*, 2019, **33**, e5204; <https://doi.org/10.1002/aoc.5204>.

35 Z. Sun, X. Chen, F. Lu, L. Zhou and Y. Zhang, *Catal. Commun.*, 2022, **162**, 106387; <https://doi.org/10.1016/j.catcom.2021.106387>.

36 A. S. Konopatsky, K. L. Firestein, N. D. Evdokimenko, A. L. Kustov, V. S. Baidyshev, I. V. Chepkasov, Z. I. Popov, A. T. Matveev, I. V. Shetinin, D. V. Leybo, I. N. Volkov, A. M. Kovalskii, D. Golberg and D. V. Shtansky, *J. Catal.*, 2021, **402**, 130; <https://doi.org/10.1016/j.jcat.2021.08.026>.

37 S. Roy, D. K. Mondal, S. Chatterjee, A. Chowdhury, T. S. Khan, M. A. Haider, S. Mandal, D. Chandra, M. Hara and A. Bhaumik, *Mol. Catal.*, 2022, **528**, 112486; <https://doi.org/10.1016/j.mcat.2022.112486>.

38 S. Hu, W. Ni, D. Yang, C. Ma, J. Zhang, J. Duan, Y. Gao and S. Zhang, *Carbon*, 2020, **162**, 245; <https://doi.org/10.1016/j.carbon.2020.02.059>.

Received: 10th October 2024; Com. 24/7645